*Biochimica et Biophysica Acta*, 641 (1981) 320—333


BBA 79134

# HEXOSE TRANSPORT IN NOVIKOFF RAT HEPATOMA CELLS

## A SIMPLE CARRIER WITH DIRECTIONAL SYMMETRY, BUT VARIABLE RELATIVE MOBILITIES OF LOADED AND EMPTY CARRIER

JON C. GRAFF *, ROBERT M. WOHLHUETER and PETER G.W. PLAGEMANN **

*Department of Microbiology, Medical School, University of Minnesota, Minneapolis, MN 55455 (U.S.A.)*

(Received August 11th, 1980)

*Key words. Hexose transport; Carrier mobility; Transport kinetics; (Novikoff rat hepatoma cell)*

## Summary

The kinetics of transport of the non-metabolizable hexose, 3-*O*-methyl-D-glucose, have been measured in Novikoff rat hepatoma cells by both zero-*trans* entry and equilibrium exchange procedures. Transport conformed to a simple carrier model which operates symmetrically with respect to direction, but with greater mobility of the loaded than of the empty carrier. Although a complete kinetic description of the transporter can, in theory, be obtained by application of integrated equations describing the time course of substrate equilibrium across the membrane beginning from the zero-*trans* situation, statistical analysis of hypothetical data indicated that directional asymmetry or differential mobilities of loaded and empty carrier cannot be discerned reliably from such data alone. The difference in mobility of loaded and empty carrier, apparent in a comparison of zero-*trans* entry and exchange data, ranged from 1.5—7-fold in different batches of cells. It is concluded that the magnitude of the difference is not an inherent property of the transporter, but is determined physiologically, and may be involved in regulation of hexose transport.

## Introduction

The kinetics of hexose transport has been studied mainly in human erythrocytes. The transporter exhibits complex kinetics and there is no general con-

* Present address: Department of Microbiology, Duke University, Durham, NC 27710, U.S.A.
** To whom correspondence should be addressed.
Abbreviation: Hepes, *N*-2-hydroxyethylpiperazine-*N'*-2-ethanesulfonic acid.

sensus on whether the simple, mobile carrier model describes the system adequately and whether more than one type of transporter is operational (for reviews, see Refs. 1 and 2). Two recent reports [3,4] suggest that the kinetic data are compatible with operation of two simple, antiparallel carriers both with directional asymmetry and differential mobilities of empty and substrate-loaded carrier *.

The kinetics of hexose transport in other types of cells, physiologically more interesting than the erythrocyte in that they appear to modulate their transport rates in response to hexose starvation [5—7], to insulin [8—12], or to viral transformation (reviewed in Ref. 13), have not been analyzed thoroughly. Such analyses have been impeded mainly by technical obstacles, chief among them obtaining adequate numbers of cells to allow accurate determination of intracellular space and substrate concentration, and the rapidity with which transmembrane equilibrium is attained. In fact, the popularity of radioactively labeled 2-deoxyglucose as model substrate for hexose transport measurements is based on the perception of it as a remedy to these problems: it is rapidly phosphorylated, but metabolized further only slowly [13,14]; the resulting deoxyglucose 6-phosphate is accumulated intracellularly to concentrations high above that of 2-deoxyglucose in the extracellular space. However, the underlying assumption — that the rate of accumulation is limited by transport — is not generally tenable [15].

In recent years methods of following transport of non-metabolizable substrates have been refined to the extent that transmembrane equilibria attained with half-times of seconds are accurately measurable in cultured cells [16,17] and dispersed adipocytes [12]. We have now applied these methods to a thorough kinetic analysis of hexose transport in cultured Novikoff rat hepatoma cells.

## Materials and Methods

*Cell culture.* Novikoff rat hepatoma cells were propagated in suspension culture in Swim's medium 67 as described previously [18,19]. Cells were enumerated with a Coulter counter and their viability was assessed by staining with trypan blue. Cultures were examined for mycoplasma contamination by the uracil/uridine incorporation method [20]. No contamination was detected.

Cells were harvested from exponential phase cultures by centrifugation and suspended at 1—4 million cells per ml in a basal medium buffered with 20 mM Hepes and free of D-glucose, but otherwise identical to BM42B [21].

*Transport measurements.* Our techniques for measuring influx of radioactively labeled substrates have been described in detail [17]. It consists of mixing cell suspension and substrate solution at short intervals with a dual syringe, delivering the mixtures sequentially into tubes containing 200 μl of a silicone

* Directional asymmetry indicates a difference in carrier mobility with respect to direction across the membrane. Greater mobility of the substrate loaded carrier than of the empty carrier is manifest as '*trans*-stimulation' or 'accelerative countertransport', and has often been so described. Carrier 'mobility' connotes some macromolecular movement, if only a conformational shift, and not necessarily carrier translocation as suggested by the term 'mobile carrier' model.

oil (density, 1.035 g/ml) and mounted in the 12-place rotor of a microcentrifuge, and then sedimenting the cells beneath the oil. The volume ratios of cell suspension to substrate depend on the cross-sectional area of the syringes employed and were typically 7.3 : 1. By these techniques segregation of cells from medium is effected within about 2 s [17], and sampling intervals of 1 s are practicable. Generally we used a schedule designed to encompass the whole time course to attainment of transmembrane equilibrium, with a predominance of points at early times (see, for example, Fig. 4).

3-*O*-[*methyl*-$^3$H]methyl-D-glucose has been used as substrate in all studies reported here. It is transported by the glucose transporter of Novikoff cells [15], but not metabolized by them. Radioactivity in the cell pellet has been corrected for that attributable to extracellular space, as measured by [*carboxy*-$^{14}$C]carboxyinulin, and normalized to intracellular water space, as measured by $^3H_2O$ [17].

These procedures were developed for measuring zero-*trans* entry but are readily extended to accommodate equilibrium exchange * and exit protocols. For exchange measurements cell suspensions were preincubated with 3-*O*-methylglucose, at a specified concentration, and sufficiently long to insure transmembrane equilibrium (about 30 min at 37°C). Suspensions were then mixed by means of the dual syringe (at 25°C) with basal medium containing the same concentrations of 3-*O*-methylglucose according to a specified schedule, and sedimented through oil. Since our technique measures cell-associated radioactivity, inward and outward exchange, though kinetically identical, are operationally distinct. i) Outward exchange was measured by introducing tracer to the cells at the time of preincubation. Cell suspension was delivered from the smaller of the two syringes, and was thus diluted 8.3-times upon mixing. In this case a decreasing cellular content of radioactivity was measured. ii) Inward exchange was measured by introducing tracer first upon mixing. Cells were delivered from the larger of the syringes, isotopic substrate from the smaller. In this case an increasing cell content of radioactivity was measured.

Analogously, for exit measurements cell suspensions were preincubated with isotopic substrate, and then delivered from the smaller syringe into medium devoid of substrate. This protocol is not zero-*trans*, in that the *trans* concentration of substrate at zero time is not zero, but 1/8.3 of the *cis* concentration.

*Statistical treatment of data.* The flux equation developed by Eilam and Stein [1] on the simple carrier model may be integrated over time to yield [22]:

$$S_{2,t} = S_1\left[1 - \exp\left(-\frac{t + (R_{21} + R_{ee}S_1/K)S_{2,t}}{KR_{oo} + R_{12}S_1 + R_{21}S_1 + S_1^2R_{ee}/K}\right)\right] \quad (1)$$

where $S_{2,t}$ = concentration of intracellular substrate at time $t$ ($S_{2,0} = 0$ for zero-*trans*); $S_1$ = extracellular concentration of substrate (and is taken as a constant); the $R$ terms are resistance factors, proportional to the time of round-trip of the

* We follow the nomenclature and symbols of Eilam and Stein [1]. 'Zero-*trans*' refers to the transfer of substrate from one side of the membrane (the *cis* side) to the other side (the *trans* side), where the concentration of substrate is, or is assumed to be, zero. 'Equilibrium exchange' refers to isotope exchange across the membrane when the chemical concentration of substrate is equal on both sides. Arbitrarily we designate the outside of the cell as side 1 and the cytoplasmic side as side 2.

carrier in each of four modes; i) loaded on the inbound trip and empty on the outbound trip ($R_{12}$); ii) empty inbound and loaded outbound ($R_{21}$); iii) loaded in both directions ($R_{ee}$); or iv) empty in both directions ($R_{oo}$). Three of these $R$ parameters are reciprocals of measurable maximum velocities, viz. $1/R_{12} = V_{12}^{zt}$ (zero-*trans* entry), $1/R_{21}^{zt} = V_{21}^{zt}$ (zero-*trans* exit) and $1/R_{ee} = V^{ee}$ (equilibrium exchange). The fourth is not directly measurable, but is calculable, since by necessity $R_{12} + R_{21} = R_{ee} + R_{oo}$. $K$ is a limit Michaelis-Menten constant, related to the several measurable Michaelis-Menten constants, for example, $K = K_{12}^{zt}R_{12}/R_{oo} = K^{ee}R_{ee}/R_{oo}$. It is identical to the 'flux ratio constant' ($R_s$) defined earlier by Regen and Morgan [23] to describe the effect of a substate on the distribution of free carrier at inner and outer faces of the membrane.

Symmetry of the carrier is expressed mathematically as equivalence of various $R$ terms. If carrier mobility is indifferent to direction, $R_{12} = R_{21}$. If the mobilities of the loaded and empty carrier are equal, $R_{ee} = R_{oo}$, and if both properties hold, all $R$ terms are equal.

Eqn. 1 is implicit in the dependent variable $S_{2,t}$. Although this form requires iterative methods for solution, we find it advantageous for purposes of least-squares regression, since the dependent variable $S_{2,t}$ is plotted directly against the independent, experimental variables $S_1$ and $t$, and the weighting problems attendant to logarithmic transformation are avoided. It will be noted that Eqn. 1 is formally similar to an integrated, first-order equation, but for the implicit term.

The time course of isotopic exchange at equilibrium is given by:

$$N_{2,t} = N_{2,\infty}\left[1 - \exp\left(-\frac{V^{ee}t}{K^{ee} + S}\right)\right] \tag{2}$$

for inward exchange, and

$$N_{2,t} = (N_{2,0} - N_{2,\infty})\exp\left(-\frac{V^{ee}t}{K^{ee} + S}\right) + N_{2,\infty} \tag{3}$$

for outward exchange. $N_{2,t}$ is the intracellular concentration of radioactivity at time $t$. (To facilitate comparison to net flux data, $N_{2,t}$ may be expressed as chemical concentration of isotopic substrate at the initial specific radioactivity.) Because of the finite dilution entailed in our method of measuring outward exchange, $N_{2,\infty}$ in Eqn. 3 is not zero.

Using a non-linear least-squares regression program, based on the algorithm of Dietrich and Rothmann [24], we fit Eqn. 1 (with specified symmetry constraints), Eqn. 2, or Eqn. 3 to the data, as appropriate to the experimental protocol used. Convergence is defined as a change of less than 0.01% in all parameter values on successive iterations. The program generates best-fitting values of the kinetic parameters, the associated standard errors of estimate, the correlation coefficient of measured values of the dependent variable on computed values ($r_{y,\hat{y}}$), and several plots depicting the individual residuals vs. the independent variables ($S_1$ and $t$) and as error distribution on a normal grid [25].

*Materials.* $^3H_2O$, [*carboxy*-$^{14}$C]carboxyinulin, and 3-*O*-[*methyl*-$^3$H]methyl-D-glucose were purchased from New England Nuclear (Boston, MA). Number

550 silicone fluid was a product of Dow Corning Corp. (Midland, MI). 3-*O*-methyl-D-glucose was obtained from Sigma Chemical Co. (St. Louis, MO).

## Results and Discussion

*The failure to discern transport asymmetry from zero-trans experiments*

The integrated rate equation for the approach to trans-membrane equilibrium in the zero-*trans* mode (Eqn. 1) contains all the kinetic parameters required to completely characterize the simple carrier. A priori one might expect to extract values for all four parameters, given a set of data embracing wide ranges of $t$ and $S_1$. These parameters would define also any directional asymmetry and differential mobilities of empty and loaded carrier. However, even with sets comprising 120 data, our program was unable to converge on the four independent parameter values. Only when the parameters to be fit could be decreased from four to two, by imposing constraints on parameter independence, were satisfactory fits obtained consistently.

To investigate systemically the inability of the statistical approach to completely characterize the transport system when the $R$ parameters are not constrained, we have resorted to Monte Carlo experiments with sets of data generated to resemble our typical hexose transport data (12 time points extending to

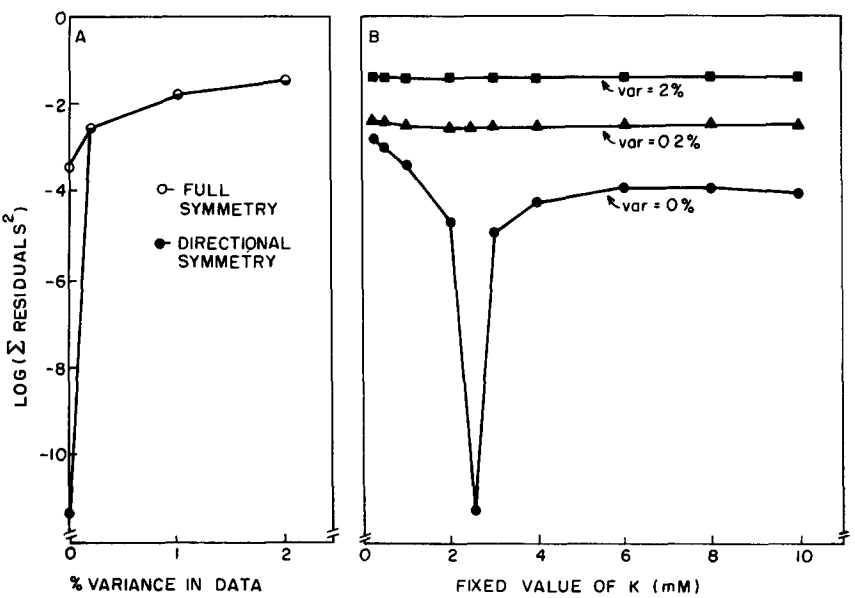


Fig. 1. Statistical evaluation of goodness-of-fit of various symmetry models to assumed transport data. Data were generated by solving Eqn. 1 at times and substrate concentrations similar to those employed in our experimental design, and at kinetic parameters resembling those for 3-*O*-methylglucose transport in Novikoff cells. Specifically, $S_1$ was taken at 1, 2, 4, 8, 16 or 32 mM; for each $S_1$ 12 values of $t$ were chosen such that the longest time represented about 90% attainment of equilibrium. Thus, $n = 72$. $K$ was taken as 2.5, $R_{12}$ ($R_{21}$) at 20, $R_{ee}$ at 5 and $R_{oo}$ at 35. Random, normally-distributed error was superimposed on the generated data corresponding to a variance of 0.2, 1 or 2%. For panel A Eqn. 1 was fitted to these data either with all $R$ terms held equal (○), or with $R_{12}$ held equal to $R_{21}$, but $R_{ee}$ and $R_{oo}$ allowed to fit independently (●). For each regression the sum of the residuals squared is plotted against the normal variance in the data. For panel B, Eqn. 1 was fitted to the same data, but all $R$ terms were allowed to fit independently, while $K$ was held at the values indicated on the abscissa.

at least 90% of equilibrium for each of six concentrations (1—32 mM), and for which $R_{12} = R_{21}$ and $R_{oo} = 7R_{ee}$ (see below)). Normally distributed error was randomly superimposed on the generated (perfect) data corresponding to variances of 0.2, 1 and 2%. Eqn. 1, with and without constraints on the $R$ parameters, was then fitted to these data sets; the results are summarized in Fig. 1.

In panel A, the sum of the residuals squared — the quantity minimized in the fitting procedure — is plotted against variance of the data for an appropriate version of the equation ($R_{12}$ held equal to $R_{21}$, $R_{oo}$ and $R_{ee}$ independent) and for an inappropriate version (all $R$ values held equal). With perfect data there was an enormous improvement of fit of the 'right' equation as compared to the 'wrong' one. With as little as 0.2% variance, however, this improvement vanished, and an $F$-test for improved fit [26] was insignificant.

Some insight into this statistical indifference to differential mobility of empty and loaded carrier (i.e. $R_{oo} = 7R_{ee}$) can be gained from Fig. 1B. The sum of the squared residuals constitutes a four-dimensional surface, the four coordinates being the four parameters of Eqn. 1; the task of the fitting program is to find a minimum on this surface. In Fig. 1B a cross-section through this surface along the $K$ coordinate was obtained by fitting Eqn. 1 repeatedly while fixing parameter $K$ at various values. With the perfect data set a distinct minimum (though greater than 0 because of round-off errors) is seen corresponding to the correct value of $K$ (2.5 mM). But, again, introduction of random error obliterates the minimum, with the consequences i) that the computer's perception of the minimum becomes difficult, if possible at all (i.e. convergence is not attained within a reasonable computation time); and ii) the parameter values corresponding to a perceived minimum are associated with large standard errors of the estimate. Not obvious in Fig. 1, but apparent from further inspection of these residual surfaces, is the fact that the surface is not simply flat, but that it forms long, narrow valleys, the floors of which are virtually flat. In other words, the estimate of one parameter is strongly contingent on the estimate of another, such that misestimates of one can be compensated by misestimates in the other, while preserving a good overall fit. Error topology of this sort has been illustrated graphically by Hoare [27].

Two additional observations emerge from such Monte Carlo experiments. First, and crucial to the present study, is that if the number of parameters in Eqn. 1 is reduced to two by means of fixing the remaining parameters at their correct values, unambiguous fits are regularly achieved and yield reliable estimates of these two parameters. In the case of nucleoside transport in Novikoff cells we have justified this reduction by demonstrating the equality of $R_{12}$, $R_{21}$, $R_{ee}$ and $R_{oo}$ [22,28]. In the case of hexose transport, where $R_{12} = R_{21}$, but $R_{ee} \neq R_{oo}$ (see below), we effect the reduction by supplying an independently determined value for $R_{ee}$.

The second observation is that, even in conditions where fitting Eqn. 1 results in great uncertainty in the values of the kinetic parameters, quite reliable estimates of initial velocity of transport ($v_{12}^{zt}$) can be extracted from the progress curve. The slope of Eqn. 1 at $t = 0$ is

$$v_{12}^{zt} = \frac{S_1/R_{12}}{KR_{oo}/R_{12} + S_1} \tag{4}$$

However, the interdependence of parameter errors is reflected in the convariances among them, such that the standard error of estimate of the derived parameter $v_{12}^{zt}$ (calculated according to Cleland [29]) is relatively small. For example, in the data sets of Fig. 1, where $K$ was deliberately fixed at values from 0.1—4-times its correct value, the deviation of computed $v_{12}^{zt}$ from its correct value never exceeded 16%.

The simulations force us to the conclusion that integrated rate analysis of zero-*trans* progress curves cannot, in practice, yield a complete kinetic description of a simple transporter. In consequence, we have resorted to the more classical approach of examining 3-*O*-methylglucose transport in different experimental protocols.

*Directional symmetry of 3-O-methylglucose transport*

As a first step in characterizing the hexose transporter of Novikoff hepatoma cells we measured the zero-*trans* entry and exit of 3-*O*-methylglucose (Fig. 2A).

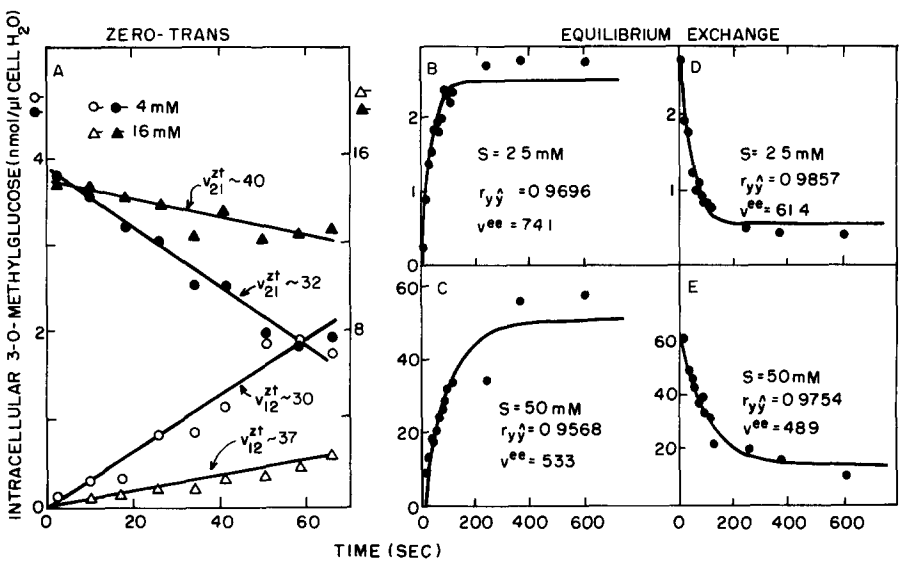


Fig. 2. Zero-*trans* entry and exit (A) and inward and outward equilibrium exchange (B—E) of 3-*O*-methylglucose in Novikoff cells at 25°C. Changes in intracellular concentration of 3-*O*-[*methyl*-$^3$H]methylglucose were measured by the rapid kinetic technique as described in Materials and Methods. Inward and outward equilibrium exchange were measured in the same population of cells. In B and C the cells were preincubated with 2.5 or 50 mM unlabeled 3-*O*-methylglucose at 37°C for 30 min. After equilibration at 25°C the accumulation of radioactivity from extracellular 3-*O*-[*methyl*-$^3$H]methylglucose at the same concentration (320 cpm/μl, irrespective of concentration) was measured. In D and E, the cells were preincubated with 2.5 or 50 mM 3-*O*-[*methyl*-$^3$H]methylglucose (2300 cpm/μl, irrespective of concentration) and then the loss of radioactivity into medium containing the same concentration of unlabeled 3-*O*-methylglucose was determined. Radioactivity/cell pellet was corrected for substrate trapped in extracellular space (1250 and 1040 cpm/pellet in (B and C) and (D and E), respectively) and converted to pmol/μl cell $H_2O$ on the basis of intracellular $H_2O$ spaces of 23.4 and 15.4 μl/pellet in (B, C) and (D, E), respectively. Eqns. 2 and 3 were fitted to the data in (B, C) and (D, E), respectively, with $K^{ee}$ fixed at 10 mM. The initial exchange velocities ($v^{ee}$) in pmol/μl cell water per s were calculated by substituting $K^{ee}$ and the estimated values of $V^{ee}$ into the following equation: $v^{ee} = V^{ee}S/(K^{ee} + S)$. Zero-*trans* entry and exit (A) were measured in another cell population by methods similar to those for equilibrium exchange, except that the cells were not preloaded with unlabeled 3-*O*-methylglucose in the entry measurements, and that exit was measured into medium devoid of unlabeled substrate. The concentrations of 3-*O*-[*methyl*-$^3$H]-methylglucose were 4 and 16 mM (50 and 12.5 cpm/nmol, respectively). The initial zero-*trans* velocities ($v_{12}^{zt}$ or $v_{21}^{zt}$) in pmol/μl cell water per s were estimated graphically as indicated.

For this purpose we restricted the interval of measurement to the first 60 s in an attempt to measure initial velocities directly, and thus to avoid the problems of choice of model and frequent lack of convergence associated with the use of integrated rate equations. For the two concentrations of substrate shown in Fig. 2A, the initial velocities of entry and exit agree within experimental error. The same conclusion followed from three other, similar experiments (not shown) encompassing a concentration range of from 1 to 40 mM. The transporter appears thus to be functionally symmetrical with respect to direction, and we are justified in simplifying Eqn. 1 by constraining $R_{12} = R_{21}$.

Panels B through E of Fig. 2 address the question of directional symmetry from a technological point of view. Theoretically, isotope exchange at equilibrium proceeds at identical rates whether measured inwards (panels B and C) or outwards (panels D and E). The comparable rates computed for inward and outward protocols thus demonstrate the reliability with which initial velocities can be extracted from progress curves measured in either direction.

*Mobilities of loaded and empty carrier*

Higher mobility of the loaded carrier in relation to that of the empty carrier is manifest in *trans*-stimulation of transport rate. Fig. 3 illustrates the *trans*-effect by way of a comparison of the rates of equilibrium exchange — whereby the *trans* concentration of 3-*O*-methylglucose equals the *cis* concentration — and entry when the *trans* concentration is initially zero. The effect was concentration dependent. as expected from a theoretical consideration of the simple carrier model, which requires a maximal effect at saturating concentrations, and no effect at limitingly low substrate concentrations.

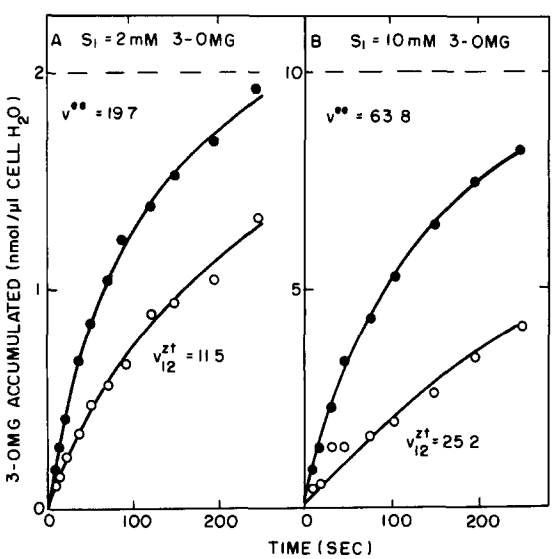


**Fig. 3. Comparison of time courses of inward equilibrium exchange and zero-*trans* entry at 2 and 10 mM 3-*O*-[*methyl*-$^3$H]methylglucose (3-OMG). The data are selected from the experiment described in detail in the legend to Fig. 4, but plotted on an expanded scale and with zero-*trans* entry and exchange data on the same coordinates. Initial velocities are expressed in pmol/µl cell $H_2O$ · s.**

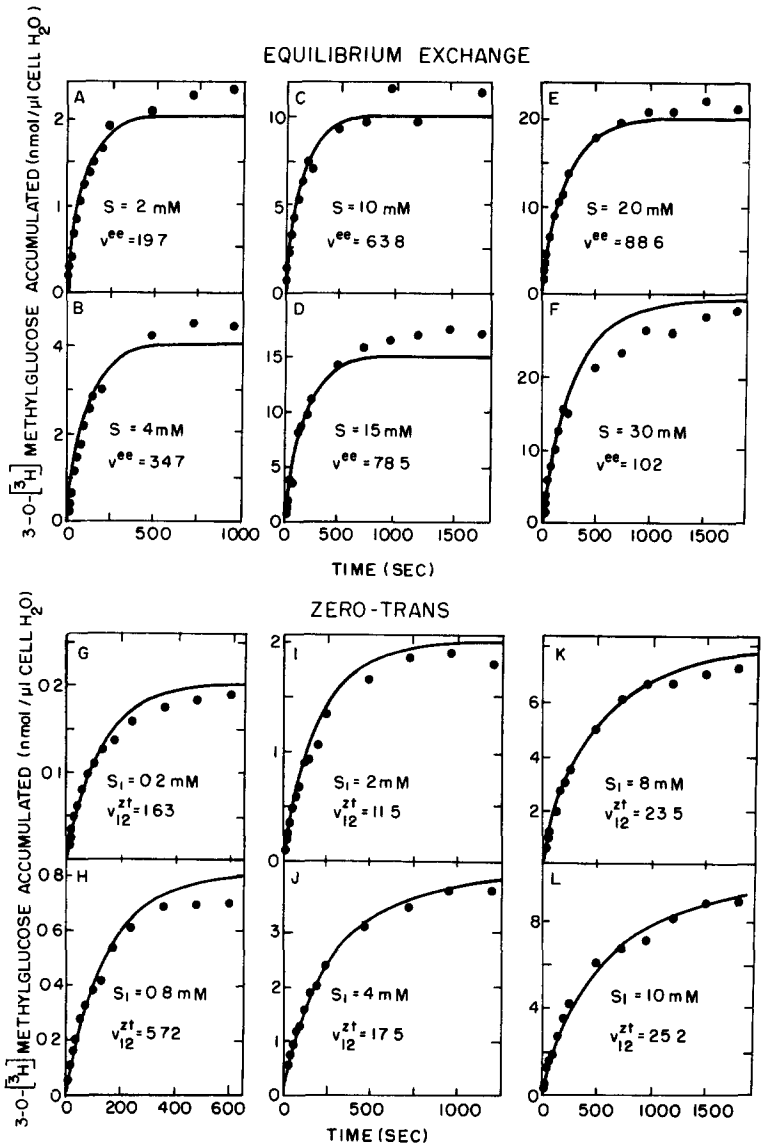


Fig. 4. Equilibrium exchange (A—F) and zero-*trans* entry (G—L) of 3-*O*-methylglucose in Novikoff rat hepatoma cells. In the equilibrium exchange protocol samples of suspension of about $2 \cdot 10^7$ cells/ml of basal medium were supplemented with 2, 4, 5, 8, 10, 15, 20 and 30 mM unlabeled 3-*O*-methylglucose, incubated at 37°C for 30 min and then equilibrated at 25°C. Time courses of radioactivity accumulation to transmembrane equilibrium from 3-*O*-[*methyl*-$^3$H]methylglucose at the same extracellular concentration as used for preloading (1280 cpm/$\mu$l, irrespective of concentration) were determined by the rapid kinetic technique as described in Materials and Methods. Zero-*trans* entry was measured in the same manner and with the same cell population, except that the cells were not preloaded with unlabeled substrate and that the extracellular 3-*O*-[*methyl*-$^3$H]methylglucose concentrations were 0.2, 0.4, 0.8, 2, 4, 6, 8 and 10 mM (1280 cpm/$\mu$l, irrespective of concentration). Radioactivity/cell pellet was corrected for radioactivity trapped in extracellular space (0.8 $\mu$l/cell pellet) and converted to pmol radioactively labeled 3-*O*-methylglucose accumulated/$\mu$l cell water on the basis of an intracellular water space of 11.6 $\mu$l/cell pellet. Eqn. 2 was fitted to the equilibrium exchange data pooled for the eight substrate concentrations. The best fitting parameters of $K^{ee}$ and $V^{ee}$ are summarized in Table I (Experiment 1). The theoretical curves for $S$ = 2, 4, 10, 15, 20 and 30 mM are presented in frames A—F. The initial velocities of equilibrium exchange ($v^{ee}$) in pmol/$\mu$l cell $H_2O \cdot s$ were calculated by substituting the computed values of $K^{ee}$ and $V^{ee}$ into the following equation: $v^{ee} = V^{ee}S/(K^{ee} + S)$. Eqn. 1 was fitted to the zero-*trans* data pooled for the eight substrate concentrations with $R_{ee}$ fixed at the value determined experimentally in the equilibrium exchange protocol (6.9 s/mM) and $R_{12}$ and $R_{21}$ held equal. The best fitting kinetic parameters are summarized in Table I (Experiment 1). The theoretical curves for $S_1$ = 0.2, 0.8, 2, 4, 8 and 10 mM are illustrated in frames G—L. The initial zero-*trans* entry velocities ($v_{12}^{zt}$) in pmol/$\mu$l cell water per s were calculated from Eqn. 4.

TABLE I

KINETIC PARAMETERS FOR THE TRANSPORT OF 3-*O*-METHYL-D-GLUCOSE IN NOVIKOFF RAT HEPATOMA CELLS

The kinetics of zero-*trans* entry and exchange were examined in 16 different batches of Novikoff rat hepatoma cells; the results of five of these are summarized here. All of the experiments were conducted analogously to that detailed in the legend to Fig. 4 (the results of which are tabulated here as Experiment 1), and encompassed six or more concentrations, generally 1, 2, 4, 8, 16 and 32 mM. Integrated rate equations were fitted to each data set, as described in the text, and the best fitting values are expressed ± S.D. of the estimate. The indented parameters were calculated directly from the fit parameters: $R_{ee} = 1/V^{ee}$, $V_{12}^{zt} = 1/R_{12}$, $K_{12}^{zt} = KR_{oo}/R_{12}$, and $K^{ee} = KR_{oo}/R_{ee}$. The intracellular and extracellular water spaces (in μl/ cell pellet) for Experiments 2—5 were: 10.4 and 3.4, 18.5 and 2.0. 24.9 and 4.4, 12.5 and 2.8, respectively.

| Experimental protocol | Parameter | Experiment number | | | | |
|---|---|---|---|---|---|---|
| | | 1 | 2 | 3 | 4 | 5 |
| Equilibrium exchange | $K^{ee}$ (mM) | 12.7 ± 1.9 | 14.3 ± 2.4 | 15.3 ± 2.6 | 17.2 ± 2.9 | 13.2 ± 1.8 |
| | $V^{ee}$ (pmol/μl cell water per s) | 145 ± 11 | 116 ± 9 | 321 ± 41 | 310 ± 28 | 342 ± 22 |
| | $r_{y,\vartheta}$ | 0.9903 | 0.9790 | 0.9691 | 0.9833 | 0.9888 |
| | $V^{ee}/K^{ee}$ ($10^3 \times s^{-1}$) | 11 | 8.1 | 21 | 18 | 26 |
| | $R_{ee}$ (s/mM) | 6.9 | 8.6 | 3.1 | 3.1 | 2.9 |
| Zero-*trans* | $R_{12} = R_{21}$ (s/mM) | 27.9 ± 0.7 | 34.0 ± 1.1 | 6.04 ± 0.53 | 5.14 ± 0.12 | 3.67 ± 0.07 |
| | $K$ (mM) | 2.4 ± 0.2 | 2.3 ± 0.2 | 3.4 ± 0.5 | 7.5 ± 0.5 | 8.5 ± 0.5 |
| | $r_{y,\vartheta}$ | 0.9966 | 0.9637 | 0.9645 | 0.9895 | 0.9920 |
| | $K_{12}^{zt} = K_{21}^{zt}$ (mM) | 4.2 | 4.1 | 5.1 | 10 | 10 |
| | $K^{ee}$ (mM) | 17 | 16 | 9.9 | 17 | 13 |
| | $V_{12}^{zt} = V_{21}^{zt}$ (pmol/μl cell water/s) | 36 | 30 | 170 | 190 | 270 |
| | $V_{12}^{zt}/K_{12}^{zt}$ ($10^3 \times s^{-1}$) | 8.5 | 7.2 | 33 | 19 | 27 |
| | $R_{oo}$ (s/mM) | 48.9 | 59.3 | 9.00 | 7.14 | 4.41 |
| | $R_{oo}/R_{ee}$ | 7.0 | 7.0 | 2.9 | 2.3 | 1.5 |

*Trans*-Acceleration is most succinctly quantitated as $R_{oo}/R_{ee}$ ratio, which, in turn, may be computed from a knowledge of $V^{ee}$ and $V_{12}^{zt}$ for a directionally symmetrical system. The experiments depicted in Fig. 4 provide this information and a good deal more. Panels A—F show representative time courses of isotopic exchange measured at eight concentrations of 3-*O*-methylglucose. Eqn. 2 was fitted to these data; the best-fitting parameters were $K^{ee} = 12.7 \pm 1.9$ mM and $V^{ee} = 145 \pm 11$ pmol/$\mu$l cell water per s. Panels G—L show time courses of 3-*O*-methylglucose equilibration in the zero-*trans* mode in the same population of cells as used for the exchange experiment. Eqn. 1 was fitted to these data whereby $R_{12}$ was held equal to $R_{21}$ and $R_{ee}$ was fixed at the value ($1/V^{ee}$ = 6.9 s/mM) obtained in the exchange experiment. Thus the unknown parameters in Eqn. 1 were reduced to two, and the regression converged at $K = 2.4 \pm 0.2$ mM and $R_{12} = R_{21} = 27.9 \pm 0.7$ s/mM, from which values were calculated: $R_{oo}$ ($=2R_{12} - R_{ee}$) = 48.9 s/mM, $V_{12}^{zt}$ ($=1/R_{12}$) = 36 pmol/$\mu$l cell water per s, $K_{12}^{zt}$ ($=KR_{oo}/R_{12}$) = 4.2 mM, and $R_{oo}/R_{ee} = 7.0$.

These results are summarized in Table I, 'Experiment 1', and support the following conclusions:

1, The Michaelis-Menten constant apparent in equilibrium exchange ($K^{ee}$) exceeded that apparent in zero-*trans* entry ($K_{12}^{zt}$) by about 3-fold. Values of the Michaelis-Menten constant $K$, which the simple carrier model requires to be independent of experimental protocol, were in fact comparable, whether obtained from zero-*trans* entry data (2.4 mM) or from exchange data ($K = K^{ee}R_{ee}/R_{oo}$ = 1.8 mM).

2, The mobility of the substrate-loaded carrier exceeded that of the empty carrier by factor 7. If we assume that the rate constants for substrate-carrier dissociation are high relative to those for carrier movement, then the return of empty carrier is rate-limiting for the zero-*trans* entry of 3-*O*-methylglucose into the cell. Translated into physiological terms, this implies that, to the extent that transport limits the rate of D-glucose metabolism and free intracellular D-glucose is maintained at a low steady-state (cf. Ref. 30), the mobility of empty carrier would be an appropriate target of physiological modulation.

3, The first-order rate constants for exchange ($V^{ee}/K^{ee}$) and zero-*trans* entry ($V_{12}^{zt}/K_{12}^{zt}$) of 3-*O*-methylglucose, as calculated from the two experimental protocols, are comparable (0.011 and 0.0085 $s^{-1}$, respectively). This attests to the internal consistency of the data and computational techniques.

4, All of the data are well accounted for by the simple carrier model.

These conclusions seem to contradict recent reports that the hexose carriers of fat cells [11,12] and rat hepatocytes [31] exhibit neither directional asymmetry nor differential mobilities of empty and loaded carrier. In the case of fat cells this claim is based on an evaluation of $K^{zt}$ from the time courses of exchange and zero-*trans* entry at a single concentration (20 mM) of 3-*O*-methylglucose. Our experience in evaluating transport data, and the Monte Carlo experiments reported above, would indicate that a single time course of substrate accumulation is grossly inadequate to define reliably the properties of a transport system. Furthermore, the data of these authors (Fig. 14 of Ref. 12) show clearly that isotope exchange occurred about twice as rapidly as zero-*trans* entry, reminiscent of our results with Novikoff cells (Fig. 3).

The apparent equality of mobility of the empty and loaded carrier of rat

hepatocytes may represent a special case of variation in $R_{oo}/R_{ee}$ ratio we observe in rat hepatoma cells (discussed below), and should be considered in context of the following section. Nevertheless, it is clear that the hexose transporters of these cells are far less complex than that of human erythrocytes [1,2]. Only 3-*O*-methylglucose transport in rat thymocytes exhibits features similar to those of the human red cell transport system in that directional asymmetry seems to be super-imposed on differential mobilities of loaded and empty carrier [32].

*Is the $R_{oo}/R_{ee}$ ratio subject to physiological modulation?*

We initiated this work under the prejudice that $R_{ee}/R_{oo}$ was an intrinsic property of the transport system, one which we wished to characterize. While there are many reports of the physiological regulation of hexose transport as a whole (see for example Refs. 7 and 13), we are not aware for any evidence that the mobilities of loaded and empty carrier are separately regulable entities. The lactose symporter of *Escherichia coli* might qualify as an example, in the sense that protonation of the carrier seems to be responsible for the more rapid movement of loaded than empty carrier [33]. Protonation, however, does not play a role in the differential mobility of the hexose carrier of Novikoff cells, since 3-*O*-methylglucose transport in these cells is not affected by pH values between 6 and 8 [34].

Over the past three years we have undertaken sixteen experiments in which, as in the experiment described above, exchange and zero-*trans* entry kinetics were compared with the same population of cells. The results of five of these are tabulated in Table I. Whereas there was considerable variation in total transport activity from cell batch to cell batch, as judged by $V^{ee}$, the Michaelis-Menten constant of exchange was fairly consistent. Most striking, however, was the variation in $R_{oo}/R_{ee}$, which ranged from 7.0 to 1.5. Because of the internal consistency of the data and their apparent conformity to the simple carrier model, we believe these differences in carrier mobility are real. Specifically, (i) The values of the correlation coefficient, $r_{y,\hat{y}}$, the reasonable magnitude of the standard errors of estimate, and our inspection of residuals (not shown) vouch for the validity of our methods of parameter estimation. (ii) The consistency of $K^{ee}$ among different batches of cells, the similarity of $V^{ee}/K^{ee}$ and $V^{zt}_{12}/K^{zt}_{12}$ within a given batch, and the similarity of $K$, whether estimated directly from zero-*trans* entry data, or computed as $K^{ee}R_{ee}/R_{oo}$ from exchange data, demonstrate the adequacy of our experimental technique.

We postulate, therefore, that differential mobilities of the loaded and empty hexose transporter are not an intrinsic characteristic of that transporter, but are contingent on the physiological state of the hepatoma cells. We do not now know what physiological factors may be involved. Neither chronological order nor the population parameters routinely determined offers any obvious correlation; in all experiments the cells were harvested from mid-to-late-exponential phase cultures with between 1.2 and 2 million cells per ml. Intracellular water space ranged from 1.2 to 1.8 $\mu$l/$10^6$ cells. The population doubling time of our Novikoff line, although not measured in the specific batches of cells used, has been reasonably invariant (9—10 h) over the years. Differences in calf serum or pancreatic autolyzate, which are constituents of the growth medium, either

TABLE II

HYPOTHETICAL GAIN IN INITIAL ZERO-*TRANS* ENTRY VELOCITY TO BE REALIZED FROM A 7-FOLD DECREASE IN RESISTIVITY TO EMPTY CARRIER

$v_{12}^{zt}$ listed in the column '$R_{oo}/R_{ee} = 7$' is calculated for a transport system with properties like those of Experiment 1 in Table I. $v_{12}^{zt}$ listed in the column '$R_{oo}/R_{ee} = 1$' is calculated for a hypothetical system of identical properties, except for $R_{oo}$, which has been decreased by a factor of 7

$$v_{12}^{zt} = \frac{2S_1/(R_{ee} + R_{oo})}{2K^{ee}R_{ee}/(R_{ee} + R_{oo}) + S_1}$$

Values for $R_{oo}/R_{ee}$ in the table represent nmol/μl cell water per s)

| Substrate concentration (mM) | $v_{12}^{zt}$ | | Gain (fold) |
|---|---|---|---|
| | $R_{oo}/R_{ee} = 7$ | $R_{oo}/R_{ee} = 1$ | |
| 0.001 | $1.14 \cdot 10^{-5}$ | $1.14 \cdot 10^{-5}$ | 1 |
| 1 | $8.66 \cdot 10^{-3}$ | $1.06 \cdot 10^{-2}$ | 1.22 |
| 2 | $1.39 \cdot 10^{-2}$ | $1.97 \cdot 10^{-2}$ | 1.41 |
| 4 | $2.01 \cdot 10^{-2}$ | $3.47 \cdot 10^{-2}$ | 1.73 |
| 8 | $2.57 \cdot 10^{-2}$ | $5.60 \cdot 10^{-2}$ | 2.18 |
| 16 | $3.00 \cdot 10^{-2}$ | $8.08 \cdot 10^{-2}$ | 2.70 |
| 200 | $3.53 \cdot 10^{-2}$ | $1.36 \cdot 10^{-1}$ | 3.86 |

with respect to hormonal factors or lipid constituents, have not been apparent, but were not monitored per se and cannot be ruled out.

The potential physiological significance of transport regulation at the level of movement of empty carrier remains in the realm of speculation. Nevertheless, some observations lend plausibility to the idea. The increases in entry ratio (against zero intracellular concentration) that might be realized by increasing mobility of the empty carrier 7-fold (to equal that of the loaded carrier) is calculated in Table II for a range of concentrations. The gain in transport velocity would approach the stimulation of 3-*O*-methylglucose influx observed upon insulin treatment of adipocytes [8—12] and of uptake of metabolizable hexoses by chick embryo fibroblasts [7] and 3T3-L1 fibroblasts [35], namely 1.5—10-fold. Such a regulatory mechanism could not, however, account for the 6-fold stimulation of $V^{ee}$ of 3-*O*-methylglucose observed by Whitesell and Gliemann [12] after insulin treatment of adipocytes. But our studies of the nucleoside transporter of Novikoff rat hepatoma and other mammalian cells [22,28] indicate that a differential mobility of empty and loaded carrier is not an inherent property of simple carriers, so that the lower mobility of the empty hexose carrier would seem to represent an unnecessary inefficiency, for which there might be a regulatory rationale.

Novikoff cells are not subject to hexose transport regulation by starvation for hexose (unpublished observations of the authors). Whether the kinetic properties of the transporters are affected by serum factors or insulin is presently under investigation. We are also currently screening other cell types with a view to identifying an experimentally manipulable hexose transporter amenable to our methods of analysis.

## Acknowledgements

The authors thank John Erbe, Patricia Wilkie, Jill Myers, and Karin Wittkop for competent technical assistance and Cheryl Thull for excellent secretarial help. This work was supported by USPHS Research Grant AM23001.

## References

1 Eilam, Y. and Stein, W.D. (1974) Meth. Membr. Biol. 2, 283—354
2 Widdas, W.F. (1980) Curr. Top. Membr. Transp. 14, 165—223
3 Eilam, Y. (1975) Biochim. Biophys. Acta 401, 364—369
4 Ginsburg, H. (1978) Biochim. Biophys. Acta 506, 119—135
5 Salter, D.W. and Cook, J.S. (1976) J. Cell. Physiol. 89, 143—156
6 Christopher, C.W., Colby, W.W. and Ullrey, D. (1976) J. Cell. Physiol. 89, 683—692
7 Musliner, T.A., Chrousos, G.P. and Amos, H. (1977) J. Cell. Physiol. 91, 155—168
8 Czech, M.P., Lawrence, J.C., Jr. and Lynn, W.S. (1974) J. Biol. Chem. 249, 5421—5427
9 Czech, M.P. (1976) J. Biol. Chem. 251, 1164—1170
10 Vinten, J., Gliemann, J. and Østerlind, K. (1976) J. Biol. Chem. 251, 794—800
11 Vinten, J. (1978) Biochim. Biophys. Acta 511, 259—273
12 Whitesell, R.R. and Gliemann, J. (1979) J. Biol. Chem. 254, 5276—5283
13 Perdue, J.F. (1978) in Virus-Transformed Cell Membranes (C. Nicolau, ed.), pp. 186—272. Academic Press, New York
14 Plagemann, P.G.W. and Richey, D.P. (1974) Biochim. Biophys. Acta 344, 263—305
15 Graff, J.C., Wohlhueter, R.M. and Plagemann, P.G.W. (1978) J. Cell. Physiol. 96, 171—188
16 Wohlhueter, R.M., Marz, R., Graff, J.C. and Plagemann, P.G.W. (1976) J. Cell. Physiol. 89, 605—612
17 Wohlhueter, R.M., Marz, R., Graff, J.C. and Plagemann, P.G.W. (1978) Meth. Cell Biol. 16, 211—236
18 Plagemann, P.G.W. and Swim, H.E. (1966) J. Bacteriol. 91, 2317—2326
19 Ward, G.A. and Plagemann, P.G.W. (1969) J. Cell. Physiol. 73, 213—231
20 Schneider, E.L., Stanbridge, E.F. and Epstein, C.J. (1974) Exptl. Cell Res. 84, 311—318
21 Plagemann, P.G.W. (1971) J. Cell. Physiol. 77, 213—240
22 Wohlhueter, R.M., Marz, R. and Plagemann, P.G.W. (1979) Biochim. Biophys. Acta 553, 262—283
23 Regen, D.M. and Morgan, H.E. (1964) Biochim. Biophys. Acta 79, 151—166
24 Dietrich, O.W. and Rothmann, O.S. (1975) Keyboard 7, 4—6
25 Draper, N.R. and Smith, H. (1966) Applied Regression Analysis. John Wiley and Sons, Inc., New York
26 Pollard, J.H. (1977) A Handbook of Numerical and Statistical Techniques, Ch. 16, Cambridge University Press, Cambridge
27 Hoare, D.J. (1972) Anal. Biochem. 46, 604—615
28 Plagemann, P.G.W. and Wohlhueter, R.M. (1980) Curr. Top. Membr. Transp. 14, 225—329
29 Cleland, W.W. (1967) Adv. Enzymol. 29, 1—32
30 Wohlhueter, R.M. and Plagemann, P.G.W. (1980) Int. Rev. Cytology 64, 171—240
31 Craik, J.D. and Elliott, K.R. (1979) Biochem. J. 182, 503—508
32 Whitesell, R.R., Tarpley, H.L. and Regen, D.M. (1977) Arch. Biochem. Biophys. 181, 596—602
33 Kaczorowski, G.J. and Kaback, H.R. (1979) Biochem. 18, 3691—3697
34 Wohlhueter, R.M. and Plagemann, P.G.W. (1980) J. Biol. Chem., in the press
35 Chang, T.H., Williams, I.H. and Polakis, S.E. (1979) Exptl. Cell Res. 120, 395—403